Resolution Dependence of the Diurnal Cycle of Precipitation Simulated by a Global Cloud-System Resolving Model

Hisashi Yashiro[1], Yoshiyuki Kajikawa[1, 2], Yoshiaki Miyamoto[1, 3], Tsuyoshi Yamaura[1], Ryuji Yoshida[1, 2], and Hirofumi Tomita[1]

[1]*RIKEN Advanced Institute for Computational Science, Kobe, Japan*
[2]*Research Center for Urban Safety and Security, Kobe University, Kobe, Japan*
[3]*Rosenstiel School of Marine and Atmospheric Science, University of Miami, Miami, Florida*

Abstract

Resolution dependence was found in the simulated diurnal precipitation cycle over land in the tropics. We conducted a series of grid refinement experiments of the atmosphere from 14 km to 0.87 km using a global high-resolution model without any convection parameterizations. In the high-resolution experiment, the peak of the cycle was earlier and precipitation at the peak was higher. The characteristics of the simulated diurnal precipitation cycle changed at a grid spacing of around 2−3 km. The precipitation started to increase in the morning in the high-resolution experiments, suggesting that small-scale moist convection became active in the late morning. In the lower-resolution experiments, convection and precipitation began in the late afternoon. As well as the enhancement of moisture transport from the boundary layer to the middle troposphere, the rapid formation of rain can also be attributed to the difference in diurnal precipitation cycles between lower and higher resolution experiments.

(**Citation**: Yashiro, H., Y. Kajikawa, Y. Miyamoto, T. Yamaura, R. Yoshida, and H. Tomita, 2016: Resolution dependence of the diurnal cycle of precipitation simulated by a global cloud-system resolving model. *SOLA*, **12**, 272−276, doi:10.2151/sola.2016-053.)

1. Introduction

Precipitation is an essential variable of climate. Heavy precipitation, which is closely associated with deep convection, is important not only for local weather stability but also for global circulation (Neale and Slingo 2003). Tropical convective systems indicate the diurnal precipitation cycle, and observations such as those from the Tropical Rainfall Measuring Mission (TRMM) have revealed the general features of the diurnal precipitation cycle in the tropics. A small peak appears in the early morning over the ocean, and a large peak appears in the late afternoon over the land (Sato et al. 2009). Many current conventional general circulation models (GCMs) do not capture this diurnal cycle of tropical precipitation, especially over land (Dai 2006). Several studies have pointed out that the problem is related to the coarse horizontal resolution and the (cumulus) convection parameterization (CP) (Neale and Slingo 2003; Dai 2006; Lee et al. 2007). A similar discrepancy in the diurnal precipitation cycle is found when comparing gridded rain gauge measurements and the Coupled Model Intercomparison Project phase 5 (CMIP5) results over the southeastern United States (Rosa and Collins 2013). The conventional GCM simulations with CP usually show the peak of the diurnal precipitation cycle around noon over land. Sensitivity studies for the CP schemes have noted that the diurnal variation can improve by changing the parameters of the scheme (Lee et al. 2007; Wang et al. 2010). A study using a 20-km mesh of high-resolution GCM with CP showed an improvement in the peak time of the diurnal precipitation cycle (Arakawa and Kitoh 2005). However, simulations using CP still contain significant uncertainty. The explicit moisture convection simulation better represents the diurnal precipitation cycle, compared to the GCM simulation with CP at the same horizontal resolution of approximately 10 km (Dirmeyer et al. 2012).

In recent years, global cloud-permitting simulations have been used to study diurnal cycles of precipitation. Global simulations with 14 km and 7 km grid spacing without CP schemes have effectively reproduced the diurnal precipitation cycle in tropical regions (Sato et al. 2009; Noda et al. 2012; Kodama et al. 2015), especially over the ocean. Nevertheless, the precipitation peak in the diurnal cycle over land occurs later than in TRMM observations. Through sensitivity experiments for the horizontal grid spacing, Sato et al. (2008, 2009) suggested that the peak precipitation time would approach that of TRMM observations with increased horizontal resolution. Another approach, which differs from the global cloud resolving simulation, was also proposed to replace the CP. The multiscale modeling framework (MMF, also known as super-parameterization) employs a high-resolution cloud-resolving model in each coarse grid (~100 km) GCM. This approach has succeeded in improving the diurnal precipitation cycle compared to conventional GCMs (e.g., Pritchard and Somerville 2009a, 2009b). However, the MMF does not explicitly express the local weather phenomena. Therefore, it is expected that the global climate and local weather are fully expressed by the global cloud-resolving simulation.

Recently, Miyamoto et al. (2013) conducted a global sub-kilometer resolution simulation. They found that a fundamental change in convection properties occurred at a grid spacing of 2−3 km as a global mean. This implies a fundamental change in the diurnal precipitation cycle. The question is, how much resolution is required for sufficient representation of the observed precipitation peak in a realistic global simulation. The purpose of this study is to clarify the resolution dependence of the diurnal variation of precipitation in the tropics, simulated by a global high-resolution model. We conducted simulations with five different horizontal resolutions. Several diagnostic variables were analyzed to show the characteristics of the temporal development of convection and precipitation.

2. Simulation settings

The model we used in this study was the non-hydrostatic icosahedral atmospheric model (NICAM, Satoh et al. 2014). The experimental settings of this study were the same as those in Miyamoto et al. (2013, 2015) and Kajikawa et al. (2016). We conducted five simulations with different horizontal grid spacing: 14 km, 7 km, 3.5 km, 1.7 km, and 0.87 km, hereafter referred to as Δ14, Δ7, Δ3.5, Δ1.7, and Δ0.87, respectively. The same land-sea distribution and terrain height were used in all experiments by interpolating from the data of Δ14. After the 3-day spin-up using coarser resolution, we conducted a 48-hour simulation. We used the output from the last 24 hours for analysis, which corresponds to one day of results from 2012082600 UTC to 2012082700 UTC. The data were sorted according to the local solar time (LST) and

Corresponding author: Hisashi Yashiro, RIKEN Advanced Institute for Computational Science, 7-1-26, Minatojima-minami-machi, Chuo-ku, Kobe, Hyogo, 650-0047, Japan. E-mail: h.yashiro@riken.jp.

were summarized according to land and ocean categories in the tropics (15°S−15°N). Details of the model and analytical method are described in Supplement 1.

3. Results and discussions

Figure 1 shows the average diurnal variation of precipitation over land and ocean in the tropics. The average diurnal precipitation cycle of August 2012, obtained from TRMM 3B42 dataset (Huffman et al. 2007), is also shown for reference. Regarding the diurnal cycle of precipitation over the ocean in the tropics (Fig. 1a), the peak times are between 0300 LST and 0600 LST in the four experiments, except for Δ14, where the peak time is delayed to approximately 0900 LST. The amplitudes of the diurnal cycle are between 1.6 and 2.1 mm day^{-1}, similar to the value of 1.3 mm day^{-1} from TRMM observations. The resolution dependence of the amplitude and timing of the precipitation peak is not clear among the four higher resolution simulations.

On the other hand, the simulated diurnal precipitation cycles over land in the tropics show a remarkable difference with horizontal resolution (Fig. 1b). The precipitation peaks appear around 2400 LST in Δ14 and Δ7. Previous studies using NICAM (Sato et al. 2009; Noda et al. 2012) also reported a midnight peak of precipitation at these resolutions. The peak time changes to around 2000 LST in Δ3.5. With increasing horizontal resolution, the peak appears earlier, and the peak amplitude becomes larger. The peak time appears at 1800 LST and 1700 LST in Δ1.7 and Δ0.87, respectively, which is equivalent to a peak time of approximately 1800 LST in TRMM 3B42 data. The peak amplitudes in the two higher resolution simulations are approximately 5 mm day^{-1}, which are slightly larger than from the TRMM observations (~3.2 mm day^{-1}). The start times of the precipitation peaks also show resolution dependence. The increase in precipitation begins in the afternoon in Δ14, Δ7, and Δ3.5. On the other hand, precipitation begins to increase in the late morning in Δ1.7 and Δ0.87. At 2400 LST and 0900 LST, the precipitation amount is relatively small, and its resolution dependence is also weak.

Figure 2 depicts the diurnal variation of the maximum vertical velocity (Wmax) and precipitable water (PW). The Wmax mainly expresses the upward motion in the cloudy area (see Supplement 1). With decreasing grid intervals, the maximum Wmax becomes larger, and the diurnal cycle appears more clearly (Fig. 2a). The minimum Wmax is also larger in the higher resolution experiments. In general, smaller grid spacing results in stronger vertical velocity with smaller horizontal scale. The clear resolution dependence of minimum Wmax suggests that relatively stronger upward motions occur throughout the day in higher resolution experiments. The peak times of Wmax become earlier, and the start times of the increasing Wmax phase appear earlier in the higher resolution experiment. The results of Δ1.7 and Δ0.87 show that convection starts before noon and rapidly increases over the following six hours. The peak time of Wmax is approximately two or three hours earlier than that of maximum precipitation (Fig. 1b). However, Δ14 shows relatively small diurnal variations, with the maximum at 2400 LST, which is almost the same as the time of peak precipitation.

The diurnal variation of PW is similar in all five experiments (Fig. 2b). The PW begins to increase around 0900 LST, in conjunction with heat and water vapor fluxes from the surface, before decreasing at around 1700 LST. The diurnal average PW increases with increasing resolution from Δ14 to Δ3.5, and Δ1.7 and Δ0.87 show similar values to Δ3.5. The change of PW from Δ14 to Δ3.5 is mainly caused by the increase of water vapor in the middle troposphere. Figure 3 shows the diurnal variation of the vertical profile of relative humidity (RH) and total hydrometeors in Δ14, Δ3.5, and Δ1.7. Drier conditions are found in Δ14 between 2 km and 6 km altitude (Fig, 3a), owing to the lower specific humidity. This difference can be related to the resolution dependence of Wmax. We speculate that the strong and small-scale upward motion contributes moisture transport from the boundary layer to the middle troposphere. The profile of RH shows a small difference between Δ3.5 and Δ1.7 (Figs. 3b and c), suggesting that vertical moisture transport and condensation become balanced at resolutions higher than Δ3.5. On the other hand, the diurnal variation of the cloud condensate profile differs significantly between Δ3.5 and Δ1.7 (Figs. 3e and f). Whereas the daily total of condensate increases from Δ14 to Δ3.5, it decreases from Δ3.5 to Δ1.7. In Δ1.7 and Δ0.87, less condensate remains in the atmosphere. At the time of total condensate increase, the hydrometeors are distributed in the lower to upper troposphere, indicating the existence of deep moist convection. The peak time appears around midnight in Δ14 (Fig. 3d) and becomes earlier in higher resolution experiments. The increase of condensate in Δ14 can be linked to the decrease of PW, which is equivalent to the decrease of RH in the middle troposphere. The results of Δ3.5 show similar characteristics to Δ14 but larger PW can result in more condensates and precipitation. For Δ1.7, the increase of precipitation starts before the time when PW begins to decrease.

Figure 4 shows the diurnal cycles of boundary layer height (BLH) and cloud base height (CBH). The maximum BLH clearly differs among the experiments (Fig. 4a). In the lower resolution simulations, the peak BLH is larger, and occurs later. The height difference reaches several hundred meters between the lowest and highest resolution experiments. For the CBH, the three experiments from Δ14 to Δ3.5 show an increase in cloud height at 1100 LST and 1500 LST, and then a decrease until 2300 LST (Fig. 4b). On the other hand, the CBHs gradually increase in experiments Δ1.7 and Δ0.87 until 0100 LST and then decrease over the following nine hours. One of the possible reasons for the difference between the two groups may be the process of precipitating convection. In the lower resolution experiments, non-precipitating clouds can be dominant, and are pushed upwards with development of the boundary layer. In the higher resolution simulations,

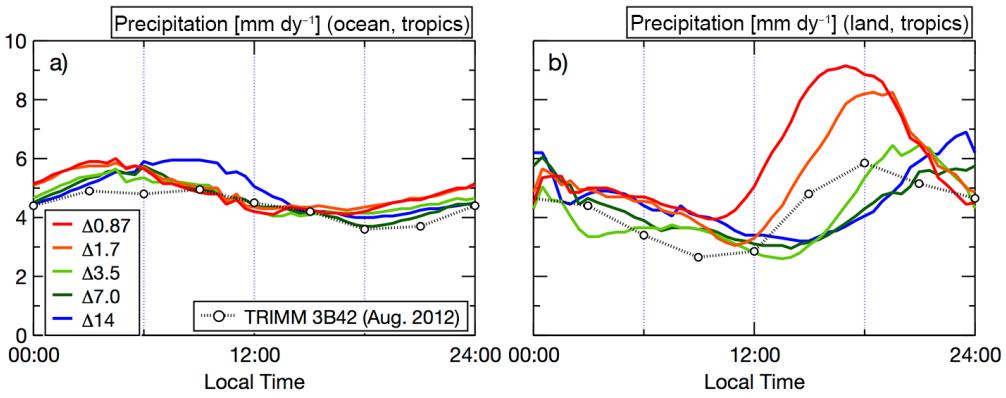

Fig. 1. Simulated diurnal cycle of precipitation in the tropics (15°S−15°N) for five horizontal resolutions: Δ14, Δ7, Δ3.5, Δ1.7, and Δ0.87. Left panel (a) is over the ocean, and right panel (b) is over land.

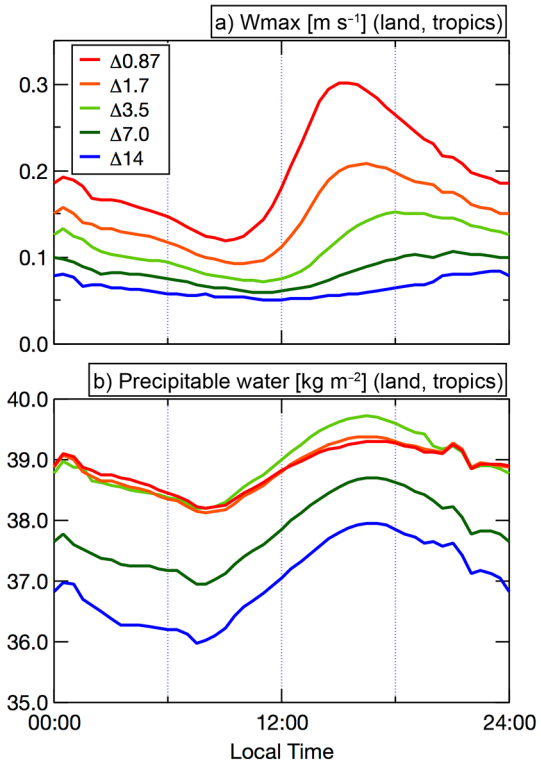

Fig. 2. Diurnal cycles of a) column maximum vertical velocity (Wmax) and b) precipitable water (PW) over land in the tropics (15°S−15°N) for five horizontal resolutions.

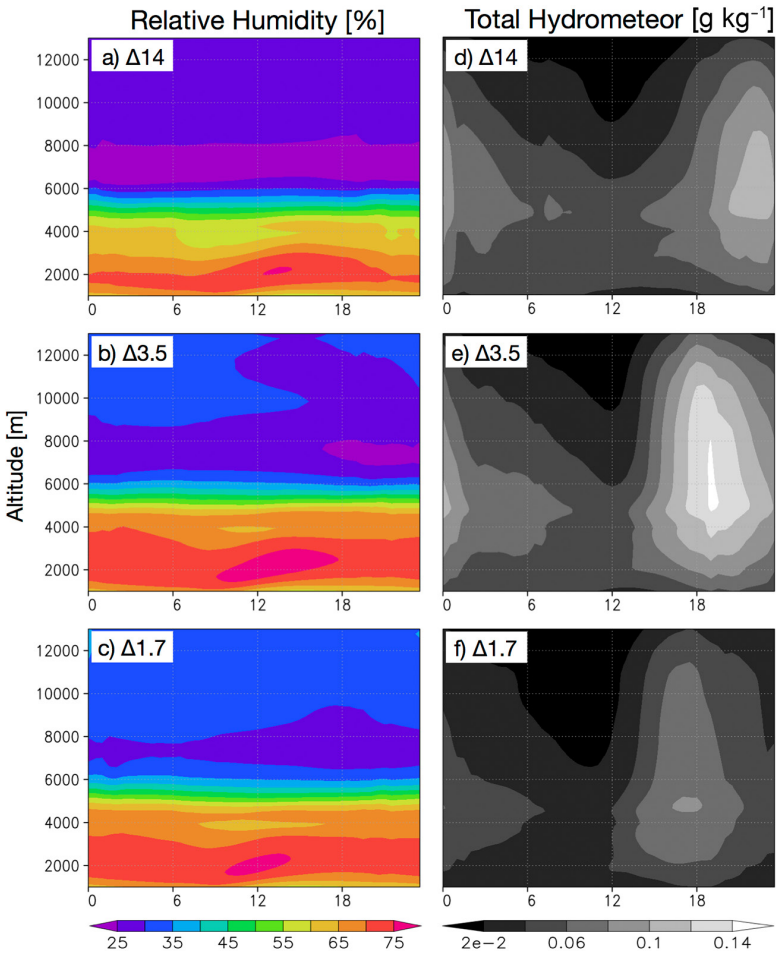

Fig. 3. Diurnal cycles of the vertical profile of relative humidity (a–c) and total hydrometeors (d–f) over land in the tropics (15°S−15°N) for Δ14, Δ3.5, and Δ1.7.

the CBH can be kept relatively lower in the morning because of the presence of convective clouds and precipitation (Fig. 1b and Fig. 2a).

The diurnal cycles of convective available potential energy (CAPE) and convection inhibition (CIN) from five experiments are shown in Fig. 5. CAPE shows a clear resolution dependence (Fig. 5a). It decreases in all experiments during the period from 1700 LST to 0600 LST, with relatively larger values in Δ14 and Δ7. Generally, simulations with larger grid spacing need more energy for grid-scale convection near the surface under the same environmental conditions. Although the PW is less apparent in the lower resolution experiments (Fig. 2b), the daily averaged CAPE is larger than in higher resolution simulations. All experiments show the increase of CAPE during the daytime. It is notable that CAPE in Δ1.7 and Δ0.87 increases more rapidly from 0600 LST to 1200 LST. Especially in Δ0.87, CAPE values close to the maximum are maintained from 1200 LST to 1700 LST, whereas single, narrow peaks appear at 1700 LST in the lower resolution experiments.

There are several potential factors that affect/change CAPE. Enhancement of the surface sensible heat flux and water vapor flux can increase CAPE, whereas increased moisture in the middle troposphere due to shallow cumulus clouds acts to decrease CAPE (Waite and Khoudier 2010). Evaporation of precipitation cools and increases moisture in the lowermost atmosphere, which tends to both increase and decrease CAPE. We speculate that local moisture convergence is a possible cause of the more rapid increase in CAPE in Δ1.7 and Δ0.87. The high-resolution simulation enables us to resolve smaller-scale convergence and divergence in connection with convection. The diurnal cycle of CIN indicates similar behavior to that of CAPE (Fig. 5b). While the maximum values of CIN are almost equal in all experiments, in the higher resolution experiments the increase in CIN is more rapid, and the peaks appear earlier. The lower resolution simulations show less negative values at nighttime.

4. Concluding remarks

Global atmospheric simulations with five different horizontal resolutions and without CP schemes showed a clear resolution dependence of the diurnal cycle of precipitation over land in the tropics. In this study, we examined the diurnal cycle of precipitation and parameters related to convective activity using the simulation results. The lower resolution simulations indicated a precipitation peak at midnight, whereas the TRMM observed precipitation peak appeared in the late afternoon. In the lowest resolution experiment, precipitating convection is initiated after the BLH decreases at approximately 1500 LST, and the precipitation peak is later than the peak of CAPE/CIN. These results suggest that moisture convection during the night is affected by orographic lift of water vapor in the two lowest resolution experiments. Kodama et al. (2015) showed the spatial distribution of precipitation peak times simulated by NICAM with a grid spacing of 14 km. In their results, midnight precipitation occurred near the mountainous areas. With increasing horizontal resolution, the peak time became earlier and the amplitude became larger. The two highest resolution experiments better reproduced the observed

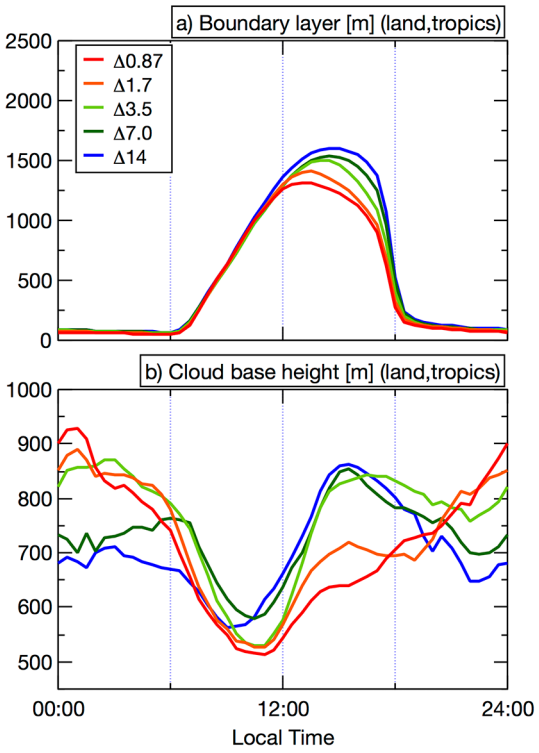

Fig. 4. Same as Fig. 2, but for a) boundary layer height (BLH) and b) cloud base height (CBH).

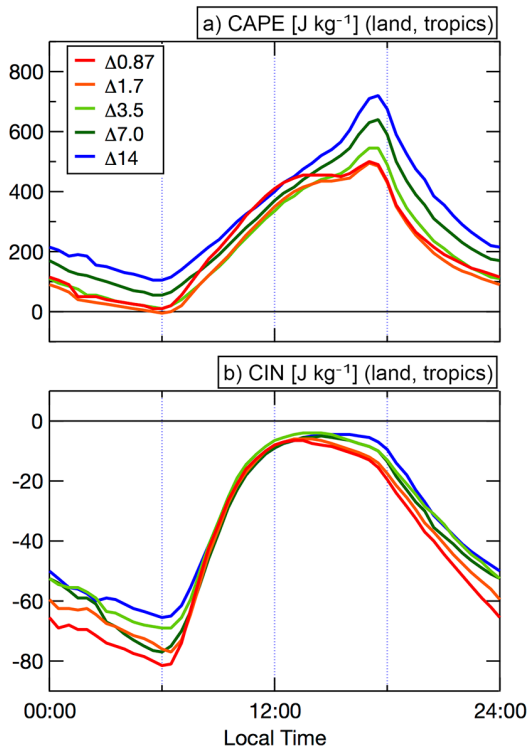

Fig. 5. Same as Fig. 2, but for a) convective available potential energy (CAPE) and b) convection inhibition (CIN).

time of peak precipitation. After sunrise, vertical velocity and precipitation in those experiments began to increase at an earlier time. Previous studies using large eddy simulation (LES) show the generation of convection in the morning, transitioning to deep convection in the afternoon (Khairoutdinov and Randall 2006; Wu et al. 2009). This process is important for effective representation of the diurnal precipitation cycle. Our results suggest that the high-resolution simulations with grid spacing of less than 2−3 km have the ability to reproduce weak convection with precipitation in the late morning. The Δ3.5 experiment showed the same RH level as Δ1.7 in the middle troposphere in the morning (Fig. 3b and c), but precipitation was not significant until the afternoon. This leads to the time difference in the precipitation peak between Δ3.5 and Δ1.7. The high-resolution simulation can effectively reproduce both small convective areas and small condensation areas. Thus, grid spacing affects not only moisture transport from the boundary layer to the middle troposphere, but also the rapid formation of rain. This fundamental change is related to the different representation of convection at resolutions less than 2−3 km, shown by Miyamoto et al. (2013) and Kajikawa et al. (2016). It is notable that the change in the diurnal precipitation cycle over land in the tropics occurs without the effect of steep and complex terrain in the high-resolution experiments.

Our study shows that improved representation of the diurnal cycle of precipitation and related variables can be achieved by increasing the horizontal resolution. However, the resolution dependence of variables can be seen even in higher resolution experiments. The resolutions used in this study are not yet sufficient to resolve all moisture convective phenomena, which require much higher resolution for the convergence of all variables. The resolution dependence of each model component also remains an issue for future study. For example, overestimation of the precipitation maximum in the higher resolution experiments is possibly caused by the lack of lateral mixing in deep convective clouds in our model (discussed in Supplement 2). Therefore, an appropriate set of schemes is required to enable better representation of the diurnal precipitation cycle.

Acknowledgements

The authors are grateful to the editor of Scientific Online Letters on the Atmosphere, and two anonymous reviewers. The authors would like to thank Akira T. Noda at the Japan Agency for Marine–Earth Science and Technology (JAMSTEC) for providing us with the compiled data of TRIMM. We would like to express our thanks to Drs. S. Nishizawa, S.A. Adachi, and Y. Sato at RIKEN Advanced Institute for Computational Science (AICS). The simulations were performed using the K computer at the RIKEN AICS. This study was supported by Strategic Programs for Innovative Research (SPIRE) Field 3 (Projection of Planet Earth Variations for Mitigating Natural Disasters), which is promoted by the Ministry of Education, Culture, Sports, Science and Technology (MEXT), Japan.

Edited by: T. Takemi

References

Arakawa, O., and A. Kitoh, 2005: Rainfall diurnal variation over the Indonesian maritime continent simulated by 20 km-mesh GCM. *SOLA*, **1**, 109−112, doi:10.2151/sola.2005-029.

Dai, A., 2006: Precipitation characteristics in eighteen coupled climate models. *J. Climate*, **19**, 4605−4630, doi:10.1175/JCLI3884.1.

Dirmeyer, P. A., B. A. Cash, J. L. Kinter III, T. Jung, L. Marx, M. Satoh, C. Stan, H. Tomita. P. Towers, N. Wedi, D. Achuthavarier, J. M. Adams, E. L. Altshuler, B. Huang, E. K. Jin, and J. Manganello, 2012: Simulating the diurnal cycle of rainfall in global climate models: Resolution versus parameterization. *Climate Dyn.*, **39**, 399−418, doi:10.1007/s00382-011-1127-9.

Huffman, G. J., D. T. Bolvin, E. J. Nelkin, D. B. Wolff, R. F. Adler, G. Gu, Y. Hong, K. P. Bowman, and E. F. Stocker, 2007: The TRMM Multisatellite Precipitation Analysis

(TMPA): Quasi-global, multiyear, Combined-sensor precipitation estimates at fine scales. *J. Hydrometeor*, **8**, 38−55, doi:10.1175/JHM560.1.

Kajikawa, Y., Y. Miyamoto, R. Yoshida, T. Yamaura, H. Yashiro, and H. Tomita, 2016: Resolution dependence of deep convections in a global simulation from over 10-kilometer to sub-kilometer grid spacing. *Prog. Earth Planet. Sci.*, **3**, 16, doi:10.1186/s40645-016-0094-5.

Kalnay, E., M. Kanamitsu, R. Kistler, W. Collins, D. Deaven, L. Gandin, M. Iredell, S. Saha, G. White, J. Woollen, Y. Zhu, A. Leetmaa, R. Reynolds, M. Chelliah, W. Ebisuzaki, W. Higgins, J. Janowiak, K. C. Mo, C. Ropelewski, J. Wang, R. Jenne, and D. Joseph, 1996: The NCEP/NCAR 40-Year Reanalysis Project. *Bull. Amer. Meteor. Soc.*, **77**, 437−471, doi:10.1175/1520-0477(1996)077<0437:TNYRP>2.0.CO;2.

Khairoutdinov, M., and D. Randall, 2006: High-resolution simulation of shallow-to-deep convection transition over land. *J. Atmos. Sci.*, **63**, 3421−3436, doi:10.1175/jas3810.1.

Lee, M.-I., S. D. Schubert, M. J. Suarez, I. M. Held, N.-C. Lau, J. J. Ploshay, A. Kumar, H.-K. Kim, and J.-K. E. Schemm, 2007: An analysis of the warm-season diurnal cycle over the continental United States and northern Mexico in general circulation models. *J. Hydrometeor*, **8**, 344−366, doi:10.1175/JHM581.1.

Miyamoto, Y., R. Yoshida, T. Yamaura, H. Yashiro, H. Tomita, and Y. Kajikawa, 2015: Does convection vary in different cloud disturbances? *Atmos. Sci. Lett.*, **16**, 305−309, doi:10.1002/asl2.558.

Miyamoto, Y., Y. Kajikawa, R. Yoshida, T. Yamaura, H. Yashiro, and H. Tomita, 2013: Deep moist atmospheric convection in a subkilometer global simulation. *Geophys. Res. Lett.*, **40**, 4922−4926, doi:10.1002/grl.50944.

Nakanishi, M., and H. Niino, 2004: An improved Mellor–Yamada level-3 model with condensation physics: Its design and verification. *Bound.-Layer Meteor.*, **112**, 1−31.

Neale, R., and J. Slingo, 2003: The maritime continent and its role in the global climate: A GCM study. *J. Climate*, **16**, 834−848, doi:10.1175/1520-0442(2003)016<0834:tmcair>2.0.co;2.

Noda, A. T., K. Oouchi, M. Satoh, and H. Tomita, 2012: Quantitative assessment of diurnal variation of tropical convection simulated by a global nonhydrostatic model without cumulus parameterization. *J. Climate*, **25**, 5119−5134, doi:10.1175/JCLI-D-11-00295.1.

Noda, A. T., K. Oouchi, M. Satoh, H. Tomita, S.-I. Iga, and Y. Tsushima, 2010: Importance of the subgrid-scale turbulent moist process: Cloud distribution in global cloud-resolving simulations. *Atmos. Res.*, **96**, 208−217, doi:10.1016/j.atmosres.2009.05.007.

Pritchard, M. S., and R. C. J. Somerville, 2009a: Assessing the diurnal cycle of precipitation in a multi-scale climate model. *J. Adv. Model. Earth Syst.*, **2**, 12, doi:10.3894/JAMES.2009.1.12.

Pritchard, M. S., and R. C. J. Somerville, 2009b: Empirical orthogonal function analysis of the diurnal cycle of precipitation in a multi-scale climate model. *Geophys. Res. Lett.*, **36**, L05812, doi:10.1029/2008GL036964.

Reynolds, R. W., N. A. Rayner, and T. M. Smith, 2002: An improved in situ and satellite SST analysis for climate. *J. Climate*, **15**, 1609−1625, doi:10.1175/1520-0442(2002)015<1609:AIISAS>2.0.CO;2.

Rosa, D., and W. D. Collins, 2013: A case study of subdaily simulated and observed continental convective precipitation: CMIP5 and multiscale global climate models comparison. *Geophys. Res. Lett.*, **40**, 5999−6003, doi:10.1002/2013GL057987.

Sato, T., H. Miura, M. Satoh, Y. N. Takayabu, and Y. Wang, 2009: Diurnal cycle of precipitation in the tropics simulated in a global cloud-resolving model. *J. Climate*, **22**, 4809−4826, doi:10.1175/2009JCLI2890.1.

Sato, T., T. Yoshinake, M. Satoh, H. Miura, and H. Fujinami, 2008: Resolution dependency of the diurnal cycle of convective clouds over the Tibetan Plateau in a mesoscale model. *J. Meteor. Soc. Japan*, **86A**, 17−31, doi:10.2151/jmsj.86A.17.

Satoh, M., and co-authors, 2014: The non-hydrostatic icosahedral atmospheric model: Description and development. *Prog. Earth Planet. Sci.*, **1**, 2293, doi:10.1186/s40645-014-0018-1.

Sekiguchi, M., and T. Nakajima, 2008: A k-distribution-based radiation code and its computational optimization for an atmospheric general circulation model. *J. Quant. Spectrosc. Radiat. Transfer*, **109**, 2779−2793, doi:10.1016/j.jqsrt.2008.07.013.

Tomita, H., 2008: New microphysical schemes with five and six categories by diagnostic generation of cloud ice. *J. Meteor. Soc. Japan*, **86A**, 121−142, doi:10.2151/jmsj.86A.121.

Uno, I., X. M. Cai, D. G. Steyn, and S. Emori, 1995: A simple extension of the Louis method for rough surface layer modelling. *Bound.-Layer Meteor.*, **76**, 395−409, doi:10.1007/BF00709241.

Waite, M. L., and B. Khouider, 2010: The deepening of tropical convection by congestus preconditioning. *J. Atmos. Sci.*, **67**, 2601−2615, doi:10.1175/2010JAS3357.1.

Wang, Y., L. Zhou, and K. Hamilton, 2007: Effect of convective entrainment/detrainment on the simulation of the tropical precipitation diurnal cycle. *Mon. Wea. Rev.*, **135**, 567−585, doi:10.1175/MWR3308.1.

Wu, C. M., B. Stevens, and A. Arakawa, 2009: What controls the transition from shallow to deep convection? *J. Atmos. Sci.*, **66**, 1793−1806, doi:10.1175/2008jas2945.1.

Manuscript received 27 June 2016, accepted 25 August 2016
SOLA: https://www.jstage.jst.go.jp/browse/sola/